Z. Physik 269, 347 – 352 (1974)


# Schematicity and Ground State Correlations in the Lead Isotopes

Stella M. Peltier* and A. Plastino**

Departamento de Física, Facultad de Ciencias Exactas, Universidad de La Plata, La Plata, Argentina

E.S. Hernández**

Departamento de Física, Facultad de Ciencias Exactas y Naturales, Universidad de Buenos Aires, Buenos Aires, Argentina

Received May 11, 1974

*Abstract.* The relationship between collectivity and ground state correlations is analyzed for the single closed shell lead isotopes. The effects of the schematic approximation are discussed, within the framework of both the quasiparticle Random Phase Approximation and the quasiparticle Tamm-Dancoff approach. The consistency of the RPA is investigated.

## 1. Introduction

In the last decade a great deal of effort has been devoted to the task of approximately describing nuclear excited states, either in the particle-hole subspace (Tamm-Dancoff, RPA) or in the two quasiparticle (q.p.) one (QTDA, QRPA), and, in all fairness, the overall results should be regarded as rather successful ones.

In later years, however, the foundations of the RPA have been subjected to careful scrutiny, and doubts about his consistency have arisen [1]. Most of the work done along these lines has been concerned with the particle-hole version of the RPA, and only recently the q.p. one has been, in this sense, specifically examined. This was done in relation with the description of collective vibrations in rare earth nuclei [2, 3].

A closely related topic is that of the approximations usually employed in order to solve the QRPA equations. In particular, the so-called schematic treatment [4] (s.t.), which assumes a separable interaction, has been widely applied (see for example Ref. 5, and works cited therein). To use this approach, one is forced to consider only the direct particle-hole (ph) term of the residual interaction. In this respect, one should carefully distinguish between its meaning in each of the two different frameworks above mentioned (i.e., particle-hole RPA and QRPA). In the last case, the s.t. implies the discard of five of the six interaction diagrams entering into the QRPA equations [6], being thus a much more drastic approximation than in the former one, in which only the exchange ph term is neglected.

It has been found in Ref. 2 that, in relation with a nonschematic description (n.s.t.), i.e., one in which the full QRPA equations are solved, without throwing away any interaction term, the s.t. exaggerates collectivity. A strong correlation was also found [3] between coherence and the detailed shape of the spectral distribution of virtual q.p. in the correlated ground state (c.g.s.). Moreover, it could be ascertained that the QRPA is consistent, either in the s.t. or in the n.s.t. [3]. All these results, however, apply to the description of collective vibrations in heavy deformed nuclei, and

* Fellow of the Comisión de Investigaciones Científicas de la Provincia de Buenos Aires, Argentina.

** Member of the Carrera del Investigador of the Consejo Nacional de Investigaciones Científicas y Técnicas of Argentina.

need not be valid generally, specially, if one considers the peculiarities of the region, i.e., stable deformed shape, definite collective character of the vibrations, high single-particle (s.p.) level density and great number of both protons and neutrons outside closed shells. The even lead isotopes constitute a natural field for discussion of the above outlined questions. They present us with just a few neutrons outside closed shells, in relatively widely spaced s.p. levels. The equilibrium shape is spherical and the collective character of the vibrations around it just begins to insinuate itself. We find then conditions that look quite antithetic to the ones that prevail in the rare earth nuclides. In addition, QRPA studies of the even-even Pb isotopes have been performed in the past utilizing both the s.t. (see for example Ref. 7) and the n.s.t. (consider for instance Ref. 8).

The purpose of the present paper is then, *in general*, to ascertain whether the characteristics of the QRPA found in Refs. 2 and 3 are inherent to the method itself (or should instead be attributed to the peculiarities of the deformed heavy regions) and, *in particular*, to answer the following questions, in relation to the description of excitations in the Pb zone:

i) Is the QRPA consistent?

ii) What is the difference between the s.t. and the n.s.t.?

iii) Is the relationship between collectivity and the structure of the c.g.s. similar to the one found in deformed heavy nuclei?

A brief review of the formalism is given in Section 2. The results are presented in Section 3 and discussed in Section 4.

## 2. Formalism

The QRPA eigenvalue problem for an excited state of angular momentum $J$ and parity $\pi$ is given by

$$\begin{bmatrix} P & Q \\ -Q & -P \end{bmatrix} \begin{bmatrix} X \\ Y \end{bmatrix} = \omega \begin{bmatrix} X \\ Y \end{bmatrix}, \tag{1}$$

where $\omega$ is the excitation energy. $P$ and $Q$ are symmetric submatrices, whose explicit expression is given in many places (see for example Ref. 9). The antisymmetrized residual interaction between q.p. yields – via the Bogoliubov Valatin transformation – six diagrams, out of which, with appropriate pairing factors, the matrices $P$ and $Q$ are built. These diagrams are depicted in Fig. 1. In the schematic approach one takes into account only the direct ph term.

The QRPA c.g.s. can be constructed by the action, upon the BCS wave function, of an operator $S$ defined as [10]

$$S = \exp\Big\{ \sum_{nJM} \sum_{iklm} C^{J\pi}_{iklm} [b_i^+ \, b_k^+]^{JM\pi} [b_l^+ \, b_m^+]^{JM\pi} \Big\}. \tag{2}$$

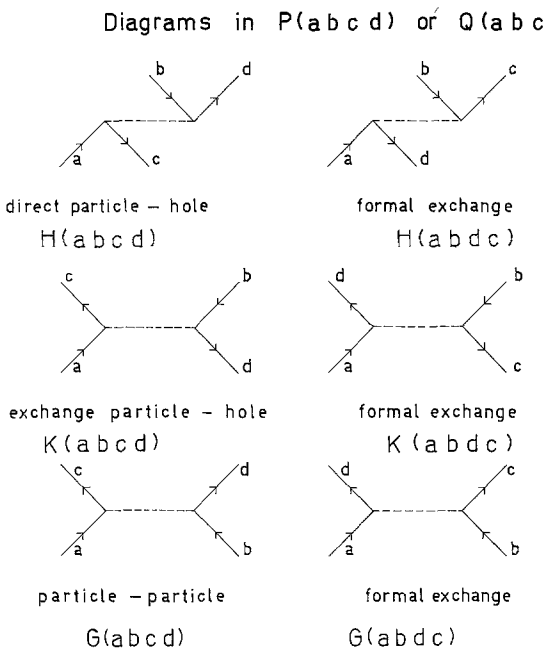


Fig. 1. The six interaction diagrams that enter into the QRPA or the QTDA equations, in building up the matrix elements $P_{abcd}$ or $Q_{abcd}$ (see Ref. 9)

The sum in (2) runs over pairs $(i\,k)$, $(l\,m)$ of q.p. operators $b$ which couple to $J$, $M$ and $\pi$. All states characterized by these last quantum numbers are to be considered. The index $n$ is used to distinguish among them. The $C$'s are the so-called correlation coefficients [10]. They can be obtained from the wave function of (1) by means of a relationship which, in matrix notation, can be stated as [10]

$$Y = CX. \tag{3}$$

One sees that, after solving the eigenvalue problem (1), it is possible to obtain the correlation coefficients by inversion, and proceed thereafter to build up explicitely, using (2), the c.g.s.

A very interesting quantity is the q.p. density matrix $\rho$, defined as

$$\rho_{ij} = \langle \text{c.g.s.} | \, b_i^+ \, b_j \, | \text{c.g.s.} \rangle, \tag{4}$$

where the diagonal elements $\rho_{ii}$ give us the average virtual population of q.p. in the s.p. level $|i\rangle$ in the c.g.s.

Evaluation of the matrix $\rho$ allows for a test of the consistency of the QRPA. A crucial assumption is made in deriving Eq. (1) (see for example Ref. 10), which can be concisely expressed as follows

$$\langle \text{c.g.s.} | \, [B_{ik}^+, B_{lm}] \, | \text{c.g.s.} \rangle \simeq \langle BCS | \, [B_{ik}^+, B_{lm}] \, | BCS \rangle, \tag{5}$$

where the $B$'s are the coupled 2 q.p. operators which appear in (2). Now, first order corrections to (5) are

linear in $\rho$ [3], so one can, after solving (1), check a posteriori the consistency of the QRPA, by going through Eqs. (3)–(2)–(4), in that order.

## 3. Results

In the present work the residual interaction has been chosen to be the Surface Delta Interaction (SDI) [8]. The s.p. scheme, interaction strength and all other numerical details are identical to those of Ref. 8. Four types of calculations were performed, which in abbreviated form are referred to as QRPA (s.t. and n.s.t.) and QTDA (s.t. and n.s.t.). Due to the fact that, for the case of the single closed shell lead isotopes, only the first excited $2^+$ states ($2_1^+$), among the low lying ones, show any sign of collectivity, attention is focused throughout on this state. Table 1 displays the energy of this state, calculated with the QRPA for the s.t. and the n.s.t. Experimental results are also shown. The quantity

$$\Delta E_1 = (E_{2^+})_{\mathrm{QRPA}} - (E_{2^+})_{\mathrm{QTDA}}, \tag{6}$$

is tabulated in Table 2, against the mass number, for both the s.t. and the n.s.t. It is seen that in both cases $\Delta E_1$ grows with $A$, but with a much greater rate in the latter one.

Fig. 2 depicts the theoretical spectra for $^{202}$Pb. (Comparison with experiment has been already made in Ref. 8, for the QTDA, n.s.t. case.) They do not look much dissimilar, although it is apparent that the QTDA calculations resemble each other more closely than the corresponding QRPA ones.

Table 1. The energies of the $2_1^+$ states in the even lead isotopes, calculated within the framework of the QRPA, for both the schematic and nonschematic cases. Experimental figures are shown in the fourth column

| $2_1^+$ Energies (MeV) | | | |
|---|---|---|---|
| Mass number | QRPA (n.s.t.) | QRPA (s.t.) | Experimental |
| 206 | 0.78 | 0.88 | 0.80 |
| 204 | 0.90 | 0.88 | 0.90 |
| 202 | 1.01 | 0.92 | 0.96 |
| 200 | 1.13 | 1.00 | 1.03 |
| 198 | 1.24 | 1.09 | 1.06 |

Table 2. Energy difference between QRPA and QTDA predictions for the $2_1^+$ state, calculated for both the schematic and nonschematic approaches

| $\Delta E_1 = (E_{2_1^+})_{\mathrm{QRPA}} - (E_{2_1^+})_{\mathrm{QTDA}}$ (MeV) | | |
|---|---|---|
| Mass number | $E$(n.s.t.) | $E$(s.t.) |
| 206 | 0.01 | 0.03 |
| 204 | 0.01 | 0.08 |
| 202 | 0.02 | 0.15 |
| 200 | 0.03 | 0.18 |
| 198 | 0.04 | 0.22 |

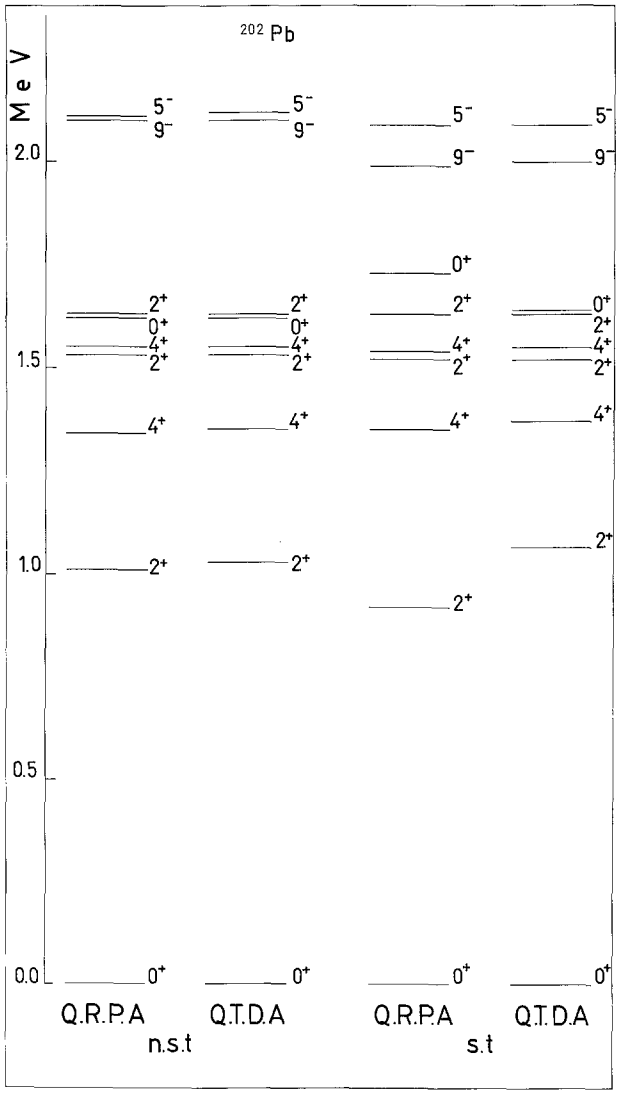


Fig. 2. Theoretical spectra for $^{202}$Pb

Another quantity of interest is

$$\Delta E_2 = E_{2^+} - E_{2\,\mathrm{q.p.}}. \tag{7}$$

In (7) $E_{2\,\mathrm{q.p.}}$ is the lowest unperturbed 2q.p. energy. $\Delta E_2$ gives us the shift produced by the residual interaction, which should be the more pronounced, the more collective the character of the corresponding excitation.

Fig. 3 exhibits the quantity $\Delta E_2$ against the mass number, for the different cases above mentioned. One clearly sees that the largest collectivity arises if one employs the s.t. within the QRPA framework. The last two pictures show also that, as far as the energetic

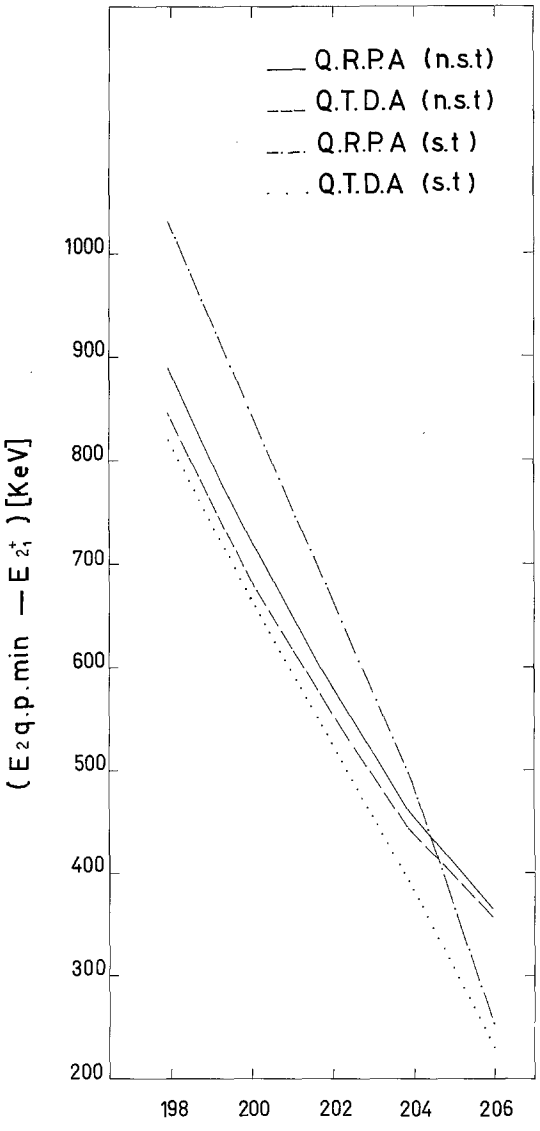


Fig. 3. For the case of the even single closed shell lead isotopes, the $2_1^+$ energy shifts from the lowest unperturbed 2 q.p. energies are plotted, for different theoretical approaches

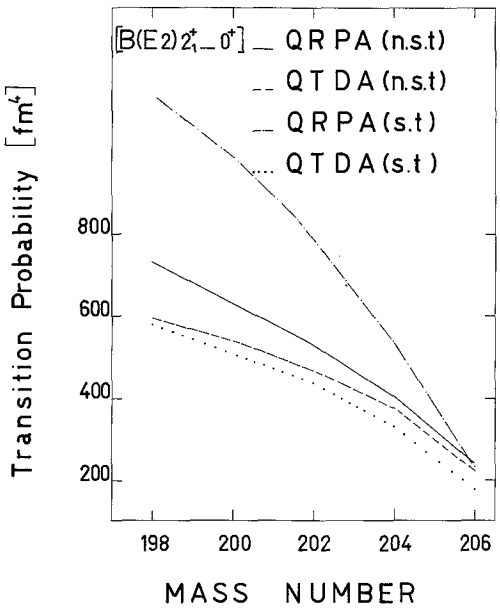


Fig. 4. $B(E2)$ transition rates into the ground state from the $2_1^+$ for the even single closed shell lead isotopes, calculated with different theoretical approaches

trend is concerned, there is a greater difference between the QRPA and QTDA within the s.t. than within the n.s.t.

Fig. 4 shows the $B(E2)$ transition rate from the ground state into the $2_1^+$. One notices that, again, the QRPA (s.t.) predicts stronger collectivity than the other types of calculation.

The quantity

$$\langle N\rangle = \sum_i \langle \text{c.g.s.}|\, b_i^+\, b_i\, |\text{c.g.s.}\rangle = \text{Tr}\,\rho, \tag{8}$$

is listed in Table 3 for both the n.s.t. and the s.t. As it can be seen from the structure of the operator $S$ in (2), the total occupation number in the c.g.s. receives contribution from all those excited states that can

Table 3. Expectation value of the quasiparticle number operator in the correlate ground state of single closed shell lead isotopes, evaluated with the nonschematic and the schematic approaches. The third column lists this number, to which all excited states contribute. The fourth one gives that fraction of the previous figure furnished by the set of collective excited states, while the one supplied by just the $2_1^+$ is displayed in the fifth column

| Total q.p. number in the correlated ground state | | | | | |
|---|---|---|---|---|---|
| Mass number | Method | Total | $2^+$ set | $2_1^+$ | $2_1^+$ percentage of total figure |
| 206 | n.s.t. | 0.069 | 0.018 | 0.010 | 15% |
| | s.t. | 0.186 | 0.142 | 0.120 | 65% |
| 204 | n.s.t. | 0.212 | 0.055 | 0.029 | 14% |
| | s.t. | 0.642 | 0.491 | 0.458 | 71% |
| 202 | n.s.t. | 0.412 | 0.108 | 0.056 | 14% |
| | s.t. | 1.13 | 0.792 | 0.756 | 67% |
| 200 | n.s.t. | 0.639 | 0.169 | 0.090 | 14% |
| | s.t. | 1.49 | 0.949 | 0.908 | 61% |
| 198 | n.s.t. | 0.848 | 0.231 | 0.128 | 14% |
| | s.t. | 1.72 | 1.00 | 0.966 | 56% |

be generated within the q.p. space. In addition to this total figure, the amounts furnished by a) the $2_1^+$ state by itself and b) the set of all $2^+$ excited states are also tabulated. A remarkable result can be observed: in the s.t., already the $2_1^+$ supplies $\langle N\rangle$ with about 65% of its total value. The corresponding percentage in the n.s.t. is a scant 14% (consider that the $2_1^+$ is the only low-lying collective excited state).

In Fig. 5 the diagonal elements of the q.p. density matrix are plotted against the q.p. energy for $^{206}$Pb.

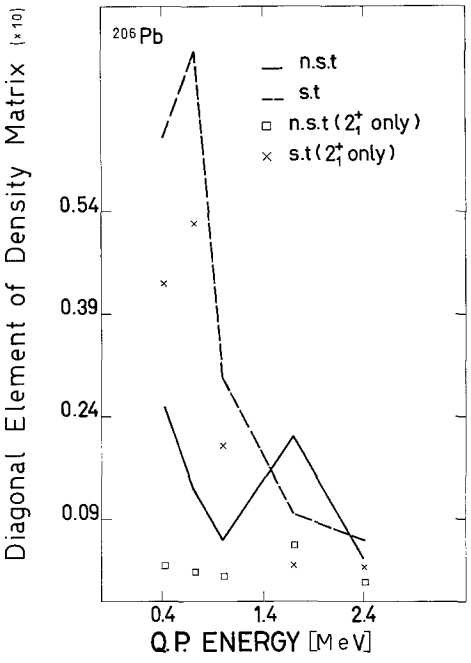


Fig. 5. Virtual q.p. spectral distribution for the correlated ground state of $^{206}$Pb

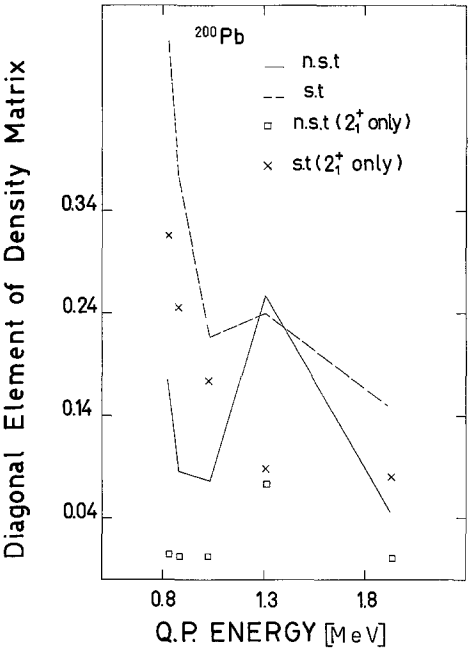


Fig. 6. Virtual q.p. spectral distribution for the correlated ground state of $^{200}$Pb

To the extreme left lies the Fermi surface. The figure illustrates the deviation of the c.g.s. from the ground state corresponding to a set of independent fermions. Both the "total" $\rho_{ii}$ (i.e., with contributions from all excited states) and that generated by just the $2_1^+$ are shown, in both the s.t. and n.s.t. cases.

Table 4. The largest diagonal elements of the density matrix are tabulated for both the nonschematic and the schematic cases

| Largest diagonal element of q.p. density matrix | | |
|---|---|---|
| Mass number | n.s.t. | s.t. |
| 206 | 0.026 | 0.075 |
| 204 | 0.076 | 0.270 |
| 202 | 0.158 | 0.443 |
| 200 | 0.255 | 0.508 |
| 198 | 0.358 | 0.486 |

The $2_1^+$ in $^{206}$Pb is not collective. Fig. 6 is similar to Fig. 5, but it refers to $^{200}$Pb, a nuclide for which the $2_1^+$ already begins to show weak traces of collectivity. The patterns depicted in these last two graphs look quantitatively different.

The largest diagonal elements of the q.p. density matrix are listed in Table 4, for both the s.t. and the n.s.t.

## 4. Discussion

The only difference between the QRPA and the QTDA lies in the fact that the former takes into account ground-state correlations (g.s.c.) while the latter does not [11]. Any discrepancies between the results obtained with either of these two methods is then attributable to the features and traits of the g.s.c.

On the other hand, dissimilitudes found between theoretical predictions made by either the s.t. or the n.s.t. are to be ascribed to the effects of the last five diagrams of Fig. 1, which the former does not consider.

As far as the energetic trends are concerned, the neglect just referred to does not seem to be a nonsensical one. In fact, the corresponding spectra do not differ too much (Fig. 2), nor are the $2_1^+$ energies widely dissimilar (Table 1).

The n.s.t. and s.t. are at variance, however, as soon as one concerns oneself with the effects of g.s.c. This can be seen already in Fig. 2. The two n.s.t. spectra (QRPA and QTDA) resemble each other more closely than the corresponding s.t. ones.

The consequences of the diverse ways of handling the g.s.c. become the more noticeable, the more collective the corresponding excited state is. The $2_1^+$ in $^{206}$Pb does not display such a character. As we move away from closed shells, increasing the number of neutron holes, collectivity begins to slowly set in, starting the $2_1^+$ states to show weak signs of it for $^{200}$Pb. The effects of the manner in which the g.s.c. are dealt with can be clearly observed in Table 2. The quantity $\Delta E_1$ of Eq. (6) is a measure of the influence that g.s.c. have upon the excitation energies. It is seen that $\Delta E_1$

grows with the hole number in both cases (n.s.t. and s.t.), but in a much more rapid fashion in the former case. All the trends described above are also apparent in Fig. 3, where the energy shift produced by the residual interaction with respect to the lowest unperturbed 2q.p. energy is shown. Again the two n.s.t. curves lie closer to each other than the corresponding s.t. ones. One notices also that the s.t. (QRPA) calculation overrates the shift with respect to the n.s.t. one. Since the $2_1^+$ comes down farther into the energy gap, the greater its collective character, we conclude that there is, within the QRPA framework, overestimation of collectivity in the s.t.

This exaggeration is distinctly displayed by the behaviour of the $B(E2)$ transition rates (Fig. 4). Since there is no collectivity in $^{206}$Pb, the way in which g.s.c. are handled becomes irrelevant, and QRPA predictions are similar for either the n.s.t. or the s.t. Coming away from closed shells, $B(E2)$ values grow, and the difference between the results of the two methods is steadily magnified.

When we focus our attention upon the specific properties of the c.g.s. we find that the virtual q.p. population also augments with the hole number. The s.t. figures are always larger than n.s.t. ones, and there is a qualitative distinction between them, which can be easily appreciated by glancing at the last column of Table 3. In the s.t. case, the c.g.s. is almost entirely built up with the correlations induced by the $2_1^+$ state. A similar result holds for the case of gamma vibrations in rare earth nuclei [3], where the band-head supply is a very large part of the whole $2^+$ contribution.

The shape of the q.p. spectral distribution (Figs. 5 and 6) allows one to draw interesting conclusions*. When there is no collectivity the s.t. and n.s.t. patterns are not yet quite defined ones. On the other hand, as the separation from closed shells becomes larger, and, correspondingly, the $B(E2)$ values grow, the above mentioned patterns adopt different forms. In the s.t. case, they exhibit an ever increasing tendency to become peaked near the Fermi surface, which, on the other hand, loses special relevance in the n.s.t. one. This behaviour is also found in the deformed heavy region [3].

It is safe to assert, as a consequence of the previous discussion, that the relationship between collectivity and the structure of the c.g.s. is similar here as that found for the case of rare earth nuclei [3], a fact that would indicate that we are, in this respect, in the presence of properties which would be inherent to the QRPA method.

* Our remarks here are based on the $2_1^+$ contribution, which is the only one that can be compared to results for the rare earth region [3].

As for the consistency question, it is convenient to consider the values displayed in Table 4, which should give us an idea as to the extent to which the assumption of Eq. (5) is a correct one. (First order corrections to the right side of (5) are linear in $\rho$.) It is seen that the QRPA is a more consistent method if the n.s.t. is adopted. The fact that, in the s.t. case, the largest diagonal element is smaller for $^{198}$Pb than for $^{200}$Pb should not be misinterpreted: there are two other diagonal elements which are also large (see Table 3). The QRPA could be regarded as consistent, as far as the n.s.t. is concerned, but doubts arise in the s.t. case, for the nuclides $^{200}$Pb and $^{198}$Pb.

The authors are very indebted to Prof. A. Faessler for helpful comments. Fruitful discussions with Dr. O. Civitaresse are also acknowledged. The staff of the Computer Centre of the Universidad de La Plata (CESPI) is thanked for allowing the use of its computing facilities.

## References

1. Goswami, A., Pal, M.K.: Nucl. Phys. **44**, 294 (1963)
   Sanderson, E.A.: Phys. Letters **19**, 141 (1965)
   Rowe, D.J.: Phys. Rev. **175**, 1283 (1968)
   Parikh, J.C., Rowe, D.J.: Phys. Rev. **175**, 1293 (1968)
   Johnson, R.E., Dreizler, R.M., Klein, A.: Phys. Rev. **186**, 1289 (1969)
   Agassi, D., Gillet, V., Lumbroso, A.: Nucl. Phys. A**130**, 129 (1969)
   Gmitrova, E., Gmitro, M., Gambhir, J.C.: Preprint IC/70/146
   Da Providencia, J., Weneser, J.: Phys. Rev. C**1**, 825 (1970)
   Ellis, P.J.: Nucl. Phys. A**155**, 625 (1970)
   Schalow, G., Yamamura, M.: Nucl. Phys. A**161**, 93 (1971)
2. Hernandez, E.S., Plastino, A.: Phys. Rev. C**5**, 1888 (1972)
3. Hernandez, E.S., Plastino, A.: Z. Physik **268**, 337 (1974)
4. Brown, G.E., Bolsterli, M.: Phys. Rev. Lett. **3**, 472 (1959)
5. Bes, D.R., Sorensen, R.A.: Advances in Nuclear Physics, Vol. 2, p. 129, edited by Baranger, M., Vogt, E., New York: Plenum Press 1969
6. Faessler, A., Plastino, A., Moszkowski, S.A.: Phys. Rev. **156**, 1064 (1967)
7. Lombard, R.J., Campi-Benet, X.: Nucl. Phys. **83**, 303 (1966)
8. Plastino, A., Arvieu, R., Moszkowski, S.A.: Phys. Rev. **145**, 837 (1966)
9. Arvieu, R.: Thesis. Ann. Phys. (Paris) **8**, 407 (1963)
10. Rowe, D.J.: Nuclear Collective Motion. Methuen and Co, 1970, Chapter 14
11. Baranger, M.: Phys. Rev. **120**, 957 (1960)

Lic. Stella M. Peltier
Prof. Dr. A. Plastino
Departamento de Física
Facultad de Ciencias Exactas
Universidad de La Plata
C.C. 67, La Plata, Argentina

Dr. E.S. Hernández
Departamento de Física
Facultad de Ciencias Exactas y Naturales
Universidad de Buenos Aires
Buenos Aires, Argentina